Plant Physiology and Biochemistry 139 (2019) 697–706

Contents lists available at ScienceDirect

Plant Physiology and Biochemistry

journal homepage: www.elsevier.com/locate/plaphy

Research article

Integration of metabolome and transcriptome analyses highlights soybean roots responding to phosphorus deficiency by modulating phosphorylated metabolite processes

Xiaohui Mo, Mengke Zhang, Cuiyue Liang, Luyu Cai, Jiang Tian*

Root Biology Center, State Key Laboratory for Conservation and Utilization of Subtropical Agro-Bioresources, College of Natural Resources and Environment, South China Agricultural University, Guangzhou, 510642, PR China

ARTICLE INFO

Keywords:
Transcriptome
Metabolome
Soybean
P deficiency

ABSTRACT

Phosphorus (P) is a major constituent of biomolecules in plant cells, and is an essential plant macronutrient. Low phosphate (Pi) availability in soils is a major constraint on plant growth. Although a complex variety of plant responses to Pi starvation has been well documented, few studies have integrated both global transcriptome and metabolome analyses to shed light on molecular mechanisms underlying metabolic responses to P deficiency. This study is the first time to investigate global profiles of metabolites and transcripts in soybean (*Glycine max*) roots subjected to Pi starvation through targeted liquid chromatography electrospray ionization mass spectrometry (LC-ESI-MS/MS) and RNA-sequencing analyses. This integrated analysis allows for assessing coordinated transcriptomic and metabolic responses in terms of both pathway enzyme expression and regulatory levels. Between two Pi availability treatments, a total of 155 metabolites differentially accumulated in soybean roots, of which were phosphorylated metabolites, flavonoids and amino acids. Meanwhile, a total of 1644 differentially expressed genes (DEGs) were identified in soybean roots, including 1199 up-regulated and 445 down-regulated genes. Integration of metabolome and transcriptome analyses revealed Pi starvation responsive connection between specific metabolic processes in soybean roots, especially metabolic processes involving phosphorylated metabolites (e.g., phosphorylated lipids and nucleic acids). Taken together, this study suggests that complex molecular responses scavenging internal Pi from phosphorylated metabolites are typical adaptive strategies soybean roots employ as responses to Pi starvation. Identified DEGs will provide potential target region for future efforts to develop P-efficient soybean cultivars.

1. Introduction

Phosphorus (P) is one of crucial nutrients in plants because it is an essential component of many biomolecules in cells, such as nucleic acids, proteins, and lipids (Chiou and Lin, 2011; Liang et al., 2014; Giri et al., 2018; Ham et al., 2018; Peng et al., 2018). Therefore, plants are extremely sensitive to phosphate (Pi) starvation, with low Pi availability being a major factor limiting crop growth and yield, especially on acid soils (Chiou and Lin, 2011; Kochian et al., 2015). Since excessive application of Pi fertilizers not only leads to environmental eutrophication, but also results in depletion of global rock Pi supplies (Veneklaas et al., 2012), development of sustainable agriculture will likely require bolstering Pi fertilizer utilization efficiency in crops. This aim may be achieved through integrated efforts to optimize P management in fields and breed cultivars with high P utilization efficiency (Tian et al., 2012; Abel, 2017; Mora-Macías et al., 2017).

Plants are known to have evolved a series of morphological and physiological strategies to enhance Pi acquisition under P deficient conditions, such as remodeling of root morphology and architecture, increasing organic acid exudation and root-associated purple acid phosphatase (PAP) activities, forming symbiotic association with arbuscular mycorrhiza or other beneficial microbes (Chiou and Lin, 2011; Liang et al., 2014; Ham et al., 2018). Over the last few decades, sets of genes and proteins responsible for plant responses to Pi starvation have been functionally characterized, which has elucidated a complex Pi signaling network in plants (Chiou and Lin, 2011; Liang et al., 2014; Ham et al., 2018). For example, several key regulators, such as *phosphate starvation response 1* (*PHR1*), *ubiquitin-like modifier E3 ligase* (*PHO2*) and SPX proteins only containing SYG1/PHO81/XPR1 domains, play important roles in controlling Pi homeostasis (Wang et al., 2014; Yao et al., 2014; Abel, 2017; Mora-Macías et al., 2017; Xue et al., 2017; Ham et al., 2018). Recently, two vacuolar Pi efflux transporters in

* Corresponding author.
E-mail address: jtian@scau.edu.cn (J. Tian).

https://doi.org/10.1016/j.plaphy.2019.04.033
Received 5 March 2019; Received in revised form 25 April 2019; Accepted 25 April 2019
Available online 26 April 2019

rice (*Oryza sativa*), OsVPE1 and OsVPE2, have been suggested to participate in controlling Pi homeostasis (Xu et al., 2019). Furthermore, two other signaling pathways working through STOP1-ALMT1 and PDR2-LPR1 have been found to coordinately regulate primary root elongation under low Pi conditions mainly through effects on callose deposition and cell wall stiffening in *Arabidopsis thaliana* (Abel, 2017; Mora-Macías et al., 2017; Ham et al., 2018).

In addition to adaptive strategies for enhancing Pi acquisition efficiency, plants may also increase internal Pi utilization efficiency mainly through scavenging and conserving of internal Pi pools. Known effectors of Pi utilization efficiency include modulator of inorganic pyrophosphate (PPi) dependent glycolysis, alternative respiratory oxidases active in the mitochondrial electron transport chain and other metabolic processes (Plaxton and Tran, 2011). For example, it has been widely found that Pi starvation results in the replacement of phospholipids in cell bio-membrane by sulfo- and galacto-lipids (Plaxton and Tran, 2011; Mehra et al., 2018). Furthermore, with the aid of gas or liquid chromatography mass spectrometry (GC-MS and LC-MS) analyses, several studies have revealed global profiles of primary and secondary metabolites responding to Pi starvation in Arabidopsis, bean (*Phaseolus vulgaris*), white lupin (*Lupinus albus*), and oat (*Avena sativa*) (Hernández et al., 2007, 2009; Müller et al., 2015; Pant et al., 2015; Wang et al., 2018).

Even with three combined transcriptomic and metabolomics studies published on bean and oat, there remains a scarcity of work designed to integrate understanding of both global transcriptome and metabolome processes underlying plant responses to Pi starvation (Hernández et al., 2007, 2009; Wang et al., 2018). This leaves considerable space for shedding light on molecular mechanisms underlying observed alteration of plant metabolite responding to P deficiency. With the rapid development of high-throughput RNA sequencing technology, global transcriptomic analysis has been widely applied to investigate Pi starvation responsive genes in a diverse range of plants, such as rice (Secco et al., 2013), *Medicago truncatula* (Liese et al., 2017), cucumber (*Cucumis sativus*) (Zhang et al., 2018), soybean (Xue et al., 2018). Subsequent, functional analysis of Pi starvation responsive genes has led to further understanding of mechanisms underlying metabolic alterations in plants responsive to Pi starvation (Chiou and Lin, 2011; Liang et al., 2014; Ham et al., 2018). Nevertheless, experiments designed to observe co-occurring transcriptomes and metabolomes promise to complement existing work with clarification of previous conclusions, while also generate new insights on specific metabolites and pathways critical for plant Pi uptake and utilization efficiency.

Soybean is a valuable source of protein and vegetable oil, and is widely cultured in the world (Herridge et al., 2008). However, soybean production is often limited by low Pi availability on soils (Chen et al., 2011; Qin et al., 2011; Li et al., 2012, 2015). Soybean has been well documented for employing a wide set of morphological and physiological adaptations to P deficiency, including development of shallow root systems, increases of malate exudation and root-associated PAP activities, and symbiotic association with arbuscular mycorrhizal fungi and rhizobia (Chen et al., 2011; Qin et al., 2011; Li et al., 2012; Liang et al., 2013; Peng et al., 2018; Wu et al., 2018). Furthermore, complex molecular mechanisms underlying soybean responses to Pi starvation have been documented through genome-wide identification of Pi starvation responsive genes, along with functional characterization of Pi starvation responsive genes, such as *GmPHR25*, *GmSPX3*, *GmPT5* and *GmEXPB2* (Chen et al., 2011; Guo et al., 2011; Qin et al., 2012; Xu et al., 2013; Li et al., 2015; Peng et al., 2018; Wu et al., 2018; Xue et al., 2018). For example, *GmPHR2*5 has recently been suggested to be a critical regulator in the P signaling network, and control Pi homeostasis in soybean because it regulates transcription of a group of Pi-starvation responsive genes in soybean, including 11 *high affinity Pi transporters* (*GmPTs*) and 5 other Pi-starvation responsive genes (Xue et al., 2017). However, there remains a large gap in understanding global changes of metabolites in soybean responding to Pi starvation, as well as the underlying molecular mechanisms. In this study, integrated transcriptome and metabolome analyses were conducted to fill in gaps in understanding coordination between transcriptomic and metabolic responses to P deficiency in soybean. This will deepen the understanding of mechanisms underlying soybean adaptive strategies to P deficiency, and will, therefore, assist in efforts to make agriculture more sustainable and economical through increasing the efficiency of Pi uptake and utilization.

2. Materials and methods

2.1. Plant materials and growth conditions

In this study, soybean (*Glycine max*) genotype YC03-3 was used in the experiments. For hydroponic experiments, soybean seeds were first surface sterilized and germinated in sand. After 4 d, uniform seedlings were transplanted to nutrient solution containing 1500 μM KNO_3, 1200 μM $Ca(NO_3)_2$, 400 μM NH_4NO_3, 500 μM $MgSO_4$, 25 μM $MgCl_2$, 300 μM K_2SO_4, 300 μM $(NH_4)_2SO_4$, 1.5 μM $MnSO_4$, 1.5 μM $ZnSO_4$, 0.5 μM $CuSO_4$, 0.16 μM $(NH_4)_6Mo_7O_{24}$, 2.5 μM NaB_4O_7, and 40 μM Fe-EDTA. For high P (+P) treatment, 250 μM KH_2PO_4 was also supplied in the nutrient solution. For low P (-P) treatment 5 μM KH_2PO_4 was supplied in the nutrient solution. During the experiment, the pH value of nutrient solution was maintained between 5.8 and 6.0 by addition of diluted HCl or KOH each day. Nutrient solution was replaced weekly and aerated continuously. Shoots, leaves and roots were harvested to determine dry weight, soluble Pi concentration, total P content, root length and root surface area at 3, 6, 9, 12, 15 d after P treatments. Root length and root surface area were evaluated by the computer image analysis software (WinRhizo Pro, Regent Instruments, Quebec, Canada) after acquiring root images from a scanner (Epson, Japan). Roots were also harvested at 12 d of P treatments for RNA-seq, quantitative RT-PCR (qRT-PCR) and targeted liquid chromatography electrospray ionization mass spectrometry (LC-ESI-MS/MS) analyses. Each treatment had at least three biological replicates.

2.2. Measurement of total P content and soluble Pi concentrations

Total P content and soluble Pi concentrations were measured as described previously (Xue et al., 2018). For total P content measurements, about 0.2 g dry weight of shoots and roots from each P treatment was separately digested in H_2SO_4, and further boiled and digested until solutions became clear. For soluble Pi concentrations, about 0.1 g of fresh soybean leaves and roots were separately ground in deionized water for extraction. The supernatant was collected after centrifugation at 12,000 *g* for 30 min. Finally, Pi concentrations in the supernatant were determined by the molybdenum blue method as previously described (Murphy and Riley, 1962).

2.3. Root metabolite analysis through LC-ESI-MS/MS

Soybean roots at 12 d of P treatment were harvested for targeted LC-ESI-MS/MS analysis. Freeze-dried roots were ground to powder using a mixer mill. Approximately 100 mg of tissue powder was extracted overnight with 1.0 mL 70% aqueous methanol at 4 °C. Supernatant was absorbed and filtrated for LC-MS analysis after centrifugation at 10,000 *g* for 10 min. Samples were then analyzed using an LC-ESI-MS/MS system (HPLC, Shim-pack UFLC SHIMADZU CBM30A system; MS, Applied Biosystems 4500 Q TRAP) as described previously (Chen et al., 2013; Li et al., 2018). Briefly, for HPLC analysis, Waters ACQUITY UPLC HSS T3 C18 column (1.8 μm, 2.1 mm*100 mm) was run with gradient program set at 100:0 V/V at 0 min, 5:95 V/V at 11.0 min, 5:95 V/V at 12.0 min, 95:5 V/V at 12.1 min, and 95:5 V/V at 15.0 min. The flow rate was maintained at 0.4 mL min^{-1}. For MS analysis, ESI source temperature and ion spray voltage were set to 500 °C and 5500 V. Meanwhile curtain gas pressures were set at 55, 60, and 25

pounds per square inch (psi). Triple quadrupole (QQQ) scans were acquired as MRM experiments with collision gas (i.e., nitrogen) set to 5 psi. Differentially accumulated metabolites were screened by supervised orthogonal projection to latent structure discriminant analysis (OPLS-DA) according to the default criteria of fold change being ≥2 or ≤0.5, and the variable importance in project (VIP) being ≥1 between -P/+P treatments. Each treatment had three biological replicates.

2.4. Root transcriptome analysis through RNA-sequencing

Soybean roots at 12 d of P treatments were also collected for mRNA library construction and sequencing as described before (Xue et al., 2018). Total root RNA was isolated using Trizol reagent (Invitrogen, Carlsbad, CA, USA) according to the manufacturer's protocol. The TruSeq RNA Sample Preparation Kit was used for cDNA library preparation. These cDNA libraries were amplified and sequenced on a BGISEQ-500 platform (BGI, Shenzhen, China). Raw reads including the adaptor sequences, low quality sequences, and unknown nucleotides were filtered into clean reads using standard quality control (QC) technique. Clean reads were aligned to soybean reference genome sequences (*Glycine max*, Williams82.a2.v1) by hierarchical indexing for spliced alignment of transcripts in the HISAT2 application (Kim et al., 2015). The fragments per kilobase of transcript per million reads mapped (FPKM) method was used to calculate normalized expression levels using RNA-Seq by Expectation Maximization (RSEM) as previously described (Li and Dewey, 2011). Differentially expressed genes (DEGs) between + P and -P treatments were identified by the NOISeq method according to the default criteria of a 2-fold or greater change in expression and deviation probability values ≥ 0.7 (Tarazona et al., 2011). Kyoto Encyclopedia of Genes and Genomes (KEGG) pathway annotations were used to classify DEGs to specific biological pathways. DEGs are mapped to gene ontology (GO) terms in the database (http://www.geneontology.org/). The calculated p-value goes through Bonferroni Correction, taking corrected p-value less than 0.05 as a threshold. Gene ontology (GO) terms fulfilling this condition are defined as significantly enriched GO terms in DEGs. Each treatment had three biological replicates.

2.5. RNA extraction and qRT-PCR analysis

Total RNA of soybean roots was extracted using the RNA-Solv reagent (OMEGA Bio-tek, USA). The cDNA was synthesized using the reverse transcription kit (Promega, Madison, WI, USA) and operated according to the manuals. The qRT-PCR was performed using Go Taq qPCR Master Mix (Promega, USA) in mixes run on an Applied Biosystems StepOnePlus Real-Time PCR system (ABI, USA) with the following reaction conditions: 95 °C for 30 s, 40 cycles of 95 °C for 5 s, 60 °C for 15 s, and 72 °C for 30 s. Relative expression levels were calculated as the ratio of candidate gene expression to housekeeping gene *GmEF-1a* expression as described previously (Li et al., 2015). The primers used in this study for qRT-PCR analyses are listed in Table S1. Each treatment had four biological replicates.

2.6. Statistical analysis

Physiological data were analyzed in Microsoft Excel 2013 (Microsoft Company, USA). Significant differences between treatments were analyzed by Student's t-tests run in SPSS (version 18.0, SPSS Institute, USA). Network of genes and metabolites were constructed based on Kyoto Encyclopedia of Genes and Genomes (KEGG) pathways.

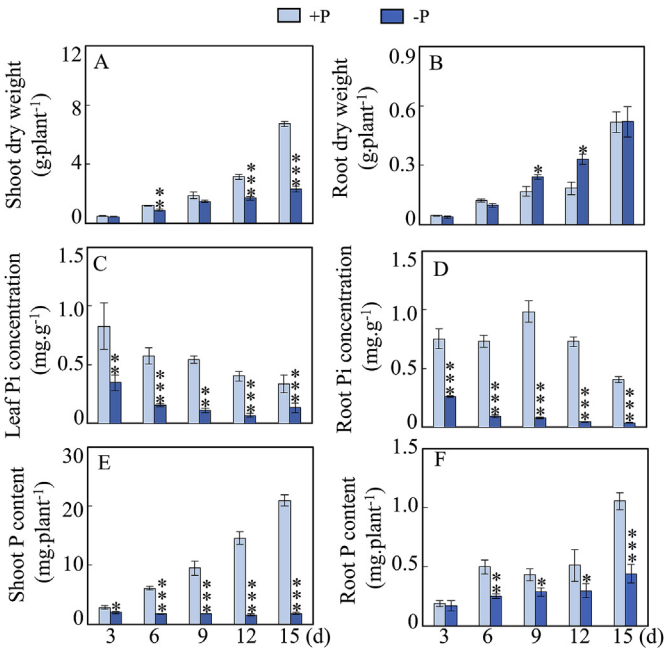

Fig. 1. Dynamic changes of soybean biomass and Pi concentration at two P levels. (A) Shoot dry weight. (B) Root dry weight. (C) Leaf soluble Pi concentration. (D) Root soluble Pi concentration. (E) Shoot P content. (F) Root P content. Data are means of four replicates with standard error bars. Asterisks indicate significant differences between + P and -P treatments in the Student's *t*-test (*: $P < 0.05$; **: $0.001 < P < 0.01$; ***: $P < 0.001$).

3. Results

3.1. Dynamic changes of soybean biomass and Pi concentration at two P levels

In order to investigate dynamic changes of soybean growth affected by Pi availability, dry weight, Pi concentration and P content in soybean were separately analyzed after 3, 6, 9, 12, and 15 d of P treatments. It was observed that soybean dry weight and Pi concentration was significantly affected by Pi availability (Fig. 1). Low Pi availability led to a decline in shoot biomass that grew increasingly evident and culminated in shoot dry weight that was 46.6% and 65.9% lower in low P conditions than in high P conditions on days 12 and 15, respectively (Fig. 1 and Fig. S1). For roots, Pi starvation resulted in significant increases in root dry weight after 9 and 12 d of P treatments, as reflected by 43.3% and 40.7% increases, respectively (Fig. 1B). However, no significant difference in root dry weight was observed between the two P treatments at 15 d (Fig. 1B). Unlike the dynamic changes of dry weight, low P treatment quickly led to significant and prolonged reductions in soluble Pi concentration in both leaves and roots (Fig. 1C and D). Similarly, except for roots at 3 d of P treatments, Pi starvation resulted in significant decreases of total P content in both shoots and roots (Fig. 1E and F).

3.2. Root length and surface area were affected by Pi starvation

Along with altering allocation to root biomass, Pi availability also affected root morphology, which was reflected by differences in both root length and root surface area between two P treatments. Low P level led to significant increases of both total root length and root surface area at 12 d, but not at other time points (Fig. 2A and B). Similarly, lateral root length was significantly greater in low P treated plants compared to those grown under high P conditions only on day of 12 (Fig. 2C). However, by 15 d, lateral root length became shorter under low P conditions (Fig. 2C). In contrast to dynamic changes observed

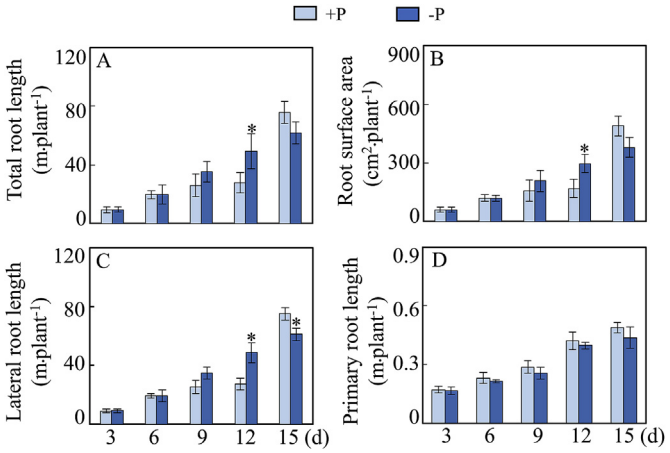

Fig. 2. Effects of Pi availability on soybean root growth. (A) Total root length. (B) Root surface area. (C) Lateral root length. (D) Primary root length. Data are means of four replicates with standard error bars. Asterisks indicate significant differences between high P (+P) and low P (-P) treatments in the Student's *t*-test (*: $P < 0.05$).

with lateral root length, primary root length was not affected by Pi starvation (Fig. 2D).

3.3. Changes of global metabolites in soybean roots at two P levels

To evaluate soybean metabolite responses to Pi starvation, metabolome analysis was performed with soybean roots after 12 d of two P treatments through targeted LC-ESI-MS/MS. A total of 531 metabolites were detected in soybean roots between two P treatments (Table 1 and Table S2). Among them, accumulation of 155 metabolites exhibited significant differences between two P treatments according to the criteria of a VIP ≥1.0 and a fold change ≥2 or ≤0.5 (Table 1 and Table S3). These metabolites participate in 20 biological pathways according to KEGG analysis (Fig. S2). Among differentially accumulated metabolites, 52 appeared to be involved in metabolic pathways, and 29 participated in and biosynthesis of secondary metabolites (Fig. S2). Furthermore, the metabolites most responsive to Pi starvation in soybean roots included 18 related to amino acids, 17 to nucleotides, 26 to flavonoids, and 36 to lipids (Table S3). For the 18 metabolites related to amino acids, 7 were found to be significantly decreased by Pi starvation, including L-aspartic acid, L-glutamic acid, L-alanine, aspartic acid di-O-glucoside, γ-Glu-Cys, S-(methyl) glutathione, and 5-oxoproline (Table S4).

3.4. Decreased accumulation of metabolites containing phosphate group

Totally, 43 metabolites containing phosphate group were significantly reduced by P deficiency in soybean roots, including 23 lipids and glycerophospholipids, 10 for nucleotides, 3 carbohydrates, 2 cholines, 1 vitamin, and 4 other metabolites (Table 2). Among them, 5 phosphorylated metabolites were detected only sparingly in soybean roots grown under low P conditions, namely sn-glycero-3-phosphocholine, O-phosphocholine, deoxyribose 5-phosphate, O-phosphorylethanolamine and Dl-glyceraldehyde 3-phosphate (Table 2). Following lipids and glycerophospholipids, the next largest group of phosphorylated metabolites affected by Pi starvation was nucleotides, which were all lower in response to Pi starvation. These nucleotides responding to Pi supplies, included adenosine 3′-monophosphate, inosine 5′-monophosphate, guanosine 5′-monophosphate, uridine 5′-diphospho-D-glucose, guanosine monophosphate, adenosine 5′-monophosphate, deoxyribose 5-phosphate, cytidine 5′-monophosphate, uridine 5′-monophosphate, guanosine 3′,5′-cyclic monophosphate (Table 2), strongly suggesting that widespread alterations in nucleotide metabolism presented in soybean responding to Pi starvation.

Table 1
Overview of metabolome and transcriptome analyses in soybean roots.

	+P	-P	Metabolites/genes with differential accumulations
Identified metabolites	531	531	155
Increased metabolites			73
Reduced metabolites			82
Identified genes	42,031	42,392	1644
Up-regulated genes			1199
Down-regulated genes			445

3.5. Flavonoid metabolites with differential accumulation in roots

A total of 108 metabolites associated with flavonoid metabolism were identified in soybean roots, including anthocyanins, flavones, flavonols, flavanones, isoflavones and flavone C-glycosides (Table S2). Among them, 26 flavonoid metabolites were differentially accumulated between two P levels, including compounds classified as anthocyanins, flavones, flavonols, flavone C-glycosides, flavanones and flavonolignan (Table S5). Several flavonoid metabolites were detected only sparingly in soybean roots grown under high P conditions, but highly induced in the low P treatment, including O-methylchrysoeriol 5-O-hexoside, quercetin, fustin, and 3,5,7,4′-tetrahydroxyflavan (afzelechin) (Table S5). In contrast, two metabolites, acetyl-eriodictyol O-hexoside and butein, were scarcer in P deficient roots than in high P roots (Table S5). Furthermore, some flavonoid metabolites in the same type exhibited different responses to Pi starvation (Table S5). For example, 2 of the 3 observed anthocyanin related metabolites were more abundant with Pi starvation, including peonidin O-hexoside and peonidin O-malonylhexoside (Table S5). At the same time, Pi starvation resulted in increased concentrations of 4 of 6 observed metabolites associated with flavones, including selgin 5-O-hexoside, O-methylchrysoeriol 5-O-hexoside, tricin 7-O-hexoside and amentoflavone (Table S5), as well as 4 of 8 flavonols, including kaempferol 3-O-glucoside, quercetin, kaempferol 3-O-galactoside and fustin (Table S5). Among flavanones, phloretin, 7-O-methyleriodictyol, pinocembrin and butein were significantly less abundant, while afzelechin was induced by Pi starvation (Table S5).

3.6. Genome-wide transcriptome analysis of soybean root responses to Pi starvation

RNA-seq analysis generated approximately 23.0 and 23.5 million clean reads in soybean roots under high and low P conditions, respectively (Table S6). About 20.6 and 20.9 million clean reads were mapped to soybean reference genes (Table S6). A total of 1644 DEGs containing 1199 up-regulated and 445 down-regulated genes were found (Table 1 and Table S7). Coefficient variations of DEGs within three biological replicates ranged from 0.71 to 0.91 at low P level, and from 0.89 to 0.96 at high P level (Table S8). KEGG analysis showed that DEGs are mainly participants in twenty pathways, of which eleven are related to metabolism processes (Fig. S3). Among the DEGs associated with these eleven metabolism related pathways, 384 are involved in global and overview maps, 155 participate in carbohydrate metabolism, and 117 function in biosynthesis of other secondary metabolites (Fig. S3).

Among the 1644 DEGs, 35 were annotated as transcription factors (TFs), including 12 *WRKY* family members and 8 MYB family members (Table S9). These transcription factor responses to Pi deprivation suggest the presence of complex regulatory network adapted to Pi starvation at the transcriptional level. Meanwhile, several gene families controlling Pi homeostasis and external organic P mobilization were also identified as responsive to Pi starvation, with examples including 11 *purple acid phosphatases* (*PAPs*), 3 *phosphate transporters* (*PTs*), 6 members of the only containing the *SYG1/PHO81/XPR1 domain* (*SPXs*),

Table 2
Identification of metabolites containing phosphate groups with reduced accumulations in soybean roots responding to P deficiency.

Compounds	+P (Intensity. cps)	-P (Intensity. cps)	Fold Change (-P/+P)	log_2 (-P/+P)
Carbohydrates				
2-Deoxyribose 1-phosphate	2.1E+06	5.2E+04	0.03	−5.31
Trehalose 6-phosphate	9.8E+04	5.4E+03	0.06	−4.17
D-Glucose 6-phosphate	1.3E+07	2.5E+05	0.02	−5.67
Cholines				
sn-Glycero-3-phosphocholine	2.8E+04	9.0E+00	0.00	−11.60
O-Phosphocholine	5.2E+05	9.0E+00	0.00	−15.81
Lipids_Glycerophospholipids				
LysoPC 16:1	3.4E+05	1.2E+05	0.34	−1.54
PC 16:1/14:1	1.0E+06	1.2E+05	0.11	−3.16
LysoPC 16:1 (2n isomer)	6.6E+06	4.0E+05	0.06	−4.06
LysoPC 18:2	4.2E+06	1.1E+06	0.26	−1.94
LysoPE 18:1 (2n isomer)	6.6E+06	4.2E+05	0.06	−3.99
LysoPC 18:1 (2n isomer)	4.0E+07	3.1E+06	0.08	−3.70
LysoPC 16:2 (2n isomer)	9.7E+05	5.2E+04	0.05	−4.23
LysoPC 18:2 (2n isomer)	3.8E+07	5.3E+06	0.14	−2.87
LysoPE 18:2 (2n isomer)	9.9E+05	2.0E+05	0.21	−2.27
LysoPE 18:0 (2n isomer)	2.1E+04	4.5E+03	0.22	−2.21
LysoPC 18:1	2.0E+05	4.5E+04	0.22	−2.16
LysoPE 18:0	4.2E+04	1.3E+04	0.30	−1.74
LysoPC 18:0 (2n isomer)	9.7E+05	2.6E+04	0.03	−5.25
LysoPE 16:0	7.1E+06	2.1E+06	0.30	−1.75
LysoPE 18:1	5.5E+06	2.9E+05	0.05	−4.24
LysoPC 20:4	8.0E+05	1.1E+05	0.14	−2.81
LysoPC 14:0 (2n isomer)	2.4E+05	1.8E+04	0.08	−3.74
LysoPC 16:0 (2n isomer)	9.8E+06	1.0E+06	0.10	−3.28
LysoPC 18:0	7.4E+06	2.0E+06	0.27	−1.91
LysoPC 20:1 (2n isomer)	5.7E+05	1.5E+04	0.03	−5.25
LysoPC 20:1	4.0E+05	5.4E+04	0.14	−2.88
LysoPE 14:0 (2n isomer)	1.1E+05	1.1E+04	0.10	−3.34
LysoPE 16:0 (2n isomer)	1.0E+07	3.3E+06	0.32	−1.66
Nucleotide and its derivates				
Adenosine 3′-monophosphate	1.1E+06	1.5E+05	0.14	−2.83
Inosine 5′-monophosphate	1.7E+05	1.9E+04	0.11	−3.16
Guanosine 5′-monophosphate	1.1E+05	1.2E+04	0.11	−3.20
Uridine 5′-diphospho-D-glucose	3.8E+07	5.9E+06	0.15	−2.69
Guanosine monophosphate	1.6E+05	1.2E+04	0.07	−3.74
Adenosine 5′-monophosphate	7.9E+05	1.2E+05	0.15	−2.72
Deoxyribose 5-phosphate	5.2E+04	9.0E+00	0.00	−12.48
Cytidine 5′-monophosphate (Cytidylic acid)	3.3E+05	1.3E+04	0.04	−4.72
Uridine 5′-monophosphate	3.2E+06	7.5E+04	0.02	−5.41
Guanosine 3′,5′-cyclic monophosphate	2.4E+05	2.6E+03	0.01	−6.53
Vitamins				
Pyridoxine 5′-phosphate	5.0E+04	1.6E+03	0.03	−4.98
Others				
2-Aminoethylphosphonate	3.1E+04	1.1E+04	0.35	−1.53
Nicotinamide adenine dinucleotide phosphate	1.5E+06	2.3E+05	0.15	−2.72
O-Phosphorylethanolamine	8.2E+04	9.0E+00	0.00	−13.15
Dl-Glyceraldehyde3-phosphate	9.2E+04	9.0E+00	0.00	−13.32

4 *ubiquitin-like modifier E3 ligase 2* members (*PHO2*), and 2 *glycerol-3-phosphate transporters* (*G3PTs*) (Table 3).

3.7. DEGs involved in flavonoid metabolism

A total of 39 DEGs could be classified as flavonoid metabolism pathways through KEGG analysis (Table S10). Moreover, increased accumulation of fustin in soybean roots subjected to Pi starvation was closely associated with increased transcription of several genes involved in fustin metabolism, including *chalcone synthase* (*CHS*), *chalcone reductase* (*CHR*), *chalcone isomerase* (*CHI*), and *flavanoid 3′-hydroxylase* (*F3′H*) (Fig. 3). Similarly, increased transcription of *leucocyanidin reductase* (*LAR*) appeared to be positively correlated with increased accumulation of both afzelechin and gallocatechin (Fig. 3). On the other hand, expression pattern of other DEGs was not apparently related to the accumulation of corresponding flavonoids. For example, transcripts of *flavonol synthase* (*FLS*) were less abundant when quercetin accumulation increased, and transcripts of both *dihydroflavonol 4-reductase* (*DFR*) and *anthocyanidin synthase* (*ANS*) decreased where an increase in the accumulation of epicatechin was observed (Fig. 3). This suggests that the DEGs might function in reactions not considered as the point of primary functionality in KEGG, or the observed accumulation of certain metabolites might result from complex processes involving multiple connected pathways.

3.8. DEGs participating in amino acid and organic acid metabolisms

A total of 66 DEGs were found to be involved in amino acid metabolism through KEGG analysis (Table S11). Among them, several DEGs were tightly integrated into metabolic processes involving several amino acids with differential accumulation observed between P treatments, including arginine, alanine, glutamate, histidine, isoleucine, leucine, and ornithine (Fig. 4). Suppression of *NADH-dependent glutamate synthase 1* (*GLT1*) transcription appeared to be related to significant decreases of glutamate in soybean roots in response to low Pi availability (Fig. 4, and Table S4, S11), while, increased transcription of *aldehyde dehydrogenase 12A1* (*ALDH12A1*) was associated with significant increases in the concentration of arginine and ornithine in soybean roots exposed to Pi starvation (Fig. 4, and Table S4, S11). Furthermore, transcripts of *malate dehydrogenase 1* (*MDH1*) and *ATP*

Table 3
Differentially expressed genes involved in Pi mobilization and homeostasis.

Gene ID	FPKM (+P)	FPKM (-P)	Fold Change (-P/+P)	Functional annotation
Gm05G138400	5.28	58.08	10.99	*Purple acid phosphatase 8*
Gm05G247900	0.17	12.59	74.04	*Purple acid phosphatase 9*
Gm05G247800	0.13	22.38	172.13	*Purple acid phosphatase 10*
Gm06G028200	0.37	10.27	27.75	*Purple acid phosphatase 11*
Gm08G056400	0.45	70.80	156.18	*Purple acid phosphatase 13*
Gm08G093500	1.94	13.95	7.18	*Purple acid phosphatase 15*
Gm08G093600	0.96	9.31	9.70	*Purple acid phosphatase 16*
Gm08G291600	6.10	16.71	2.74	*Purple acid phosphatase 17*
Gm09G229200	0.47	10.31	22.09	*Purple acid phosphatase 20*
Gm10G071000	12.12	32.44	2.68	*Purple acid phosphatase 21*
Gm12G007500	3.66	23.98	6.56	*Purple acid phosphatase 23*
Gm09G223700	15.34	102.33	6.67	*Glycerol-3-phosphate transporter 3*
Gm12G013200	1.43	36.10	25.30	*Glycerol-3- phosphate transporter 4*
Gm10G018800	5.07	16.89	3.33	*Nitrogen limitation adaptation 2*
Gm02G003700	21.41	10.31	0.48	*Ubiquitin-like modifier E3 ligase 1*
Gm07G196500	50.54	11.53	0.23	*Ubiquitin-like modifier E3 ligase 2-1*
Gm13G179600	150.29	51.62	0.34	*Ubiquitin-like modifier E3 ligase 2-2*
Gm13G239100	94.67	13.52	0.14	*Ubiquitin-like modifier E3 ligase 2-3*
Gm15G074200	25.36	6.01	0.24	*Ubiquitin-like modifier E3 ligase 2-4*
Gm03G162800	2.37	6.56	2.77	*Phosphate transporter 2*
Gm07G222700	2.48	7.84	3.16	*Phosphate transporter 3*
Gm10G006700	14.69	83.85	5.71	*Phosphate transporter 4*
Gm01G135500	1.88	78.39	41.77	*SPX domain gene 1*
Gm04G147600	0.13	32.20	241.48	*SPX domain gene 3*
Gm06G069000	1.37	9.95	7.25	*SPX domain gene 4*
Gm13G166800	7.10	107.32	15.12	*SPX domain gene 7*
Gm17G114700	5.53	158.35	28.62	*SPX domain gene 8*
Gm03G032400	0.01	50.18	5017.67	*SPX domain gene 10*
Gm09G263400	0.46	4.16	9.11	*Major Facilitator Superfamily with SPX domain-containing protein 1*

citrate (pro-S)-lyase (*ACLY*), both of which act in the tricarboxylic acid (TCA) cycle, were significantly more abundant in response to Pi starvation, suggesting that enhanced TCA metabolism might be related to decreases in aspartate and glutamate concentrations in soybean roots under low P conditions (Fig. 4, and Table S4, S7). On the other hand, significant decreases in *branched-chain amino acid aminotransferase 2* (*BCAT2*) transcription in response to Pi starvation were not correlated with increased accumulation of leucine and isoleucine (Fig. 4, and Table S4, S11), which strongly suggests that metabolic processes involving leucine and isoleucine in soybean root responses to Pi

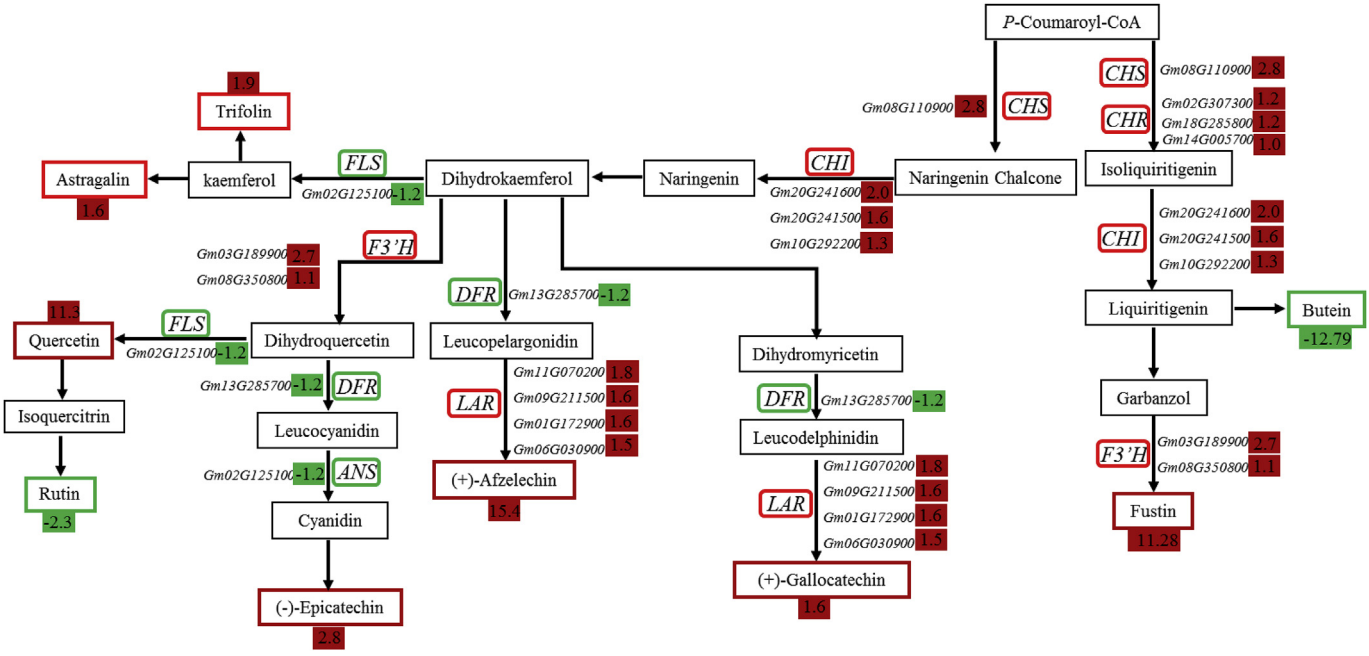

Fig. 3. Differentially expressed genes and differentially accumulated metabolites associated with flavonoid metabolism pathways. *CHS*, *chalcone synthase*; *CHR*, *chalcone reductase*; *CHI*, *chalcone isomerase*; *F3'H*, *flavanoid 3'-hydroxylase*; *DFR*, *dihydroflavonol 4-reductase*; *ANS*, *anthocyanidin synthase/leucocyanidin oxygenase*; *FLS*, *flavonol synthase*; *LAR*, *leucocyanidin reductase*. Genes that are significantly up-regulated genes and metabolites that increase in response to P deprivation are marked in red boxes, while down-regulated genes and metabolites with declining concentrations are in green boxes. Numbers indicate $\log_2$ transformed ratios of gene transcription or metabolite concentrations measured at low P (-P) and high P (+P) levels. (For interpretation of the references to colour in this figure legend, the reader is referred to the Web version of this article.)

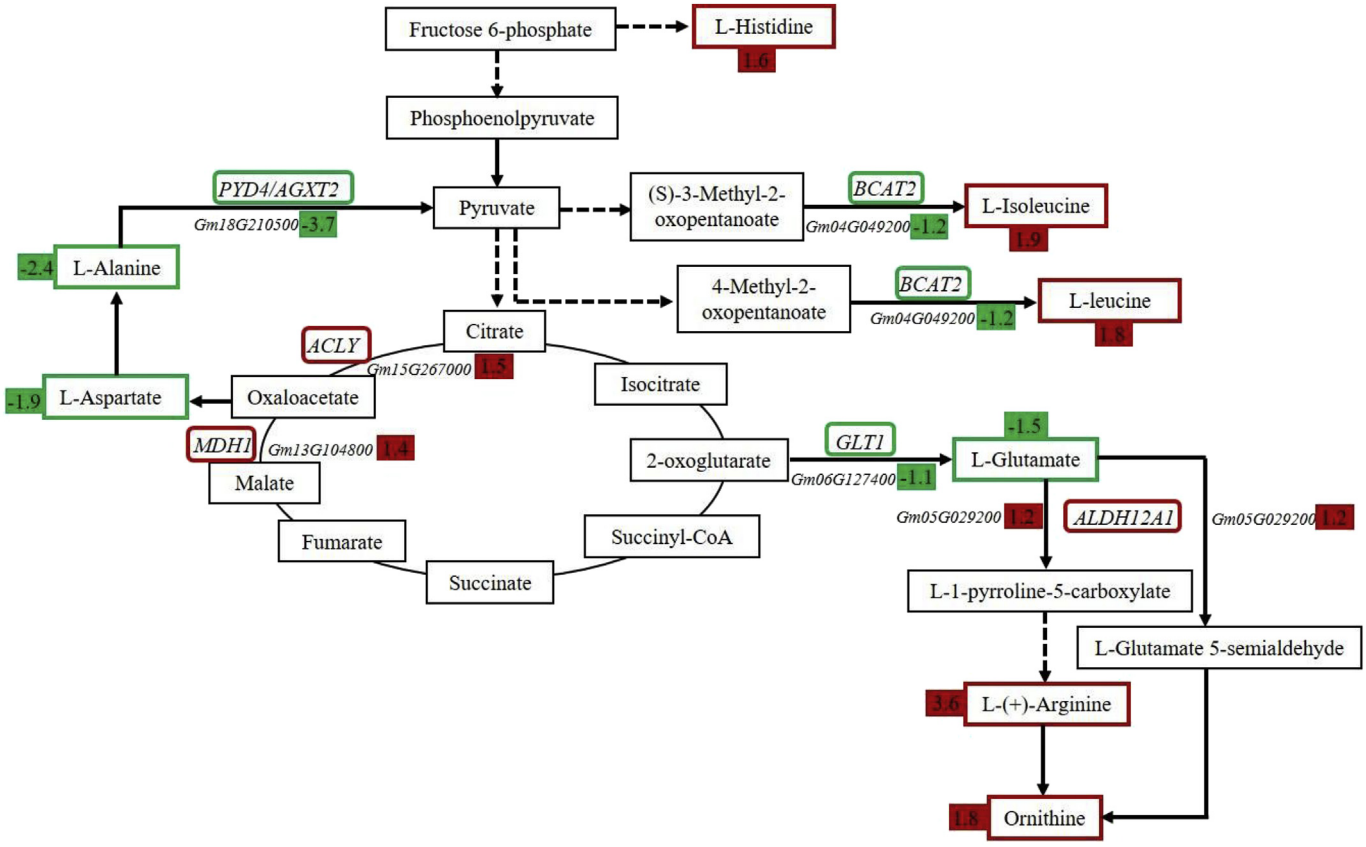

Fig. 4. Differentially expressed genes and differentially accumulated metabolites involved in organic acid and amino acid metabolism pathways. *MDH1*, *malate dehydrogenase 1*; *ACLY*, *ATP citrate (pro-S)-lyase*; *PYD4*, *pyrimidine 4*; *AGXT2*, *alanine-glyoxylate transaminase*; *BCAT2*, *branched-chain amino acid aminotransferase 2*; *GLT1*, *NADH-dependent glutamate synthase 1*; *ALDH12A1*, *aldehyde dehydrogenase 12A1*. Genes that are significantly up-regulated genes and metabolites that increase in response to P deprivation are marked in red boxes, while down-regulated genes and metabolites with declining concentrations are in green boxes. Numbers indicate $\log_2$ transformed ratios of gene transcription or metabolite concentrations measured at low P (-P) and high P (+P) levels. (For interpretation of the references to colour in this figure legend, the reader is referred to the Web version of this article.)

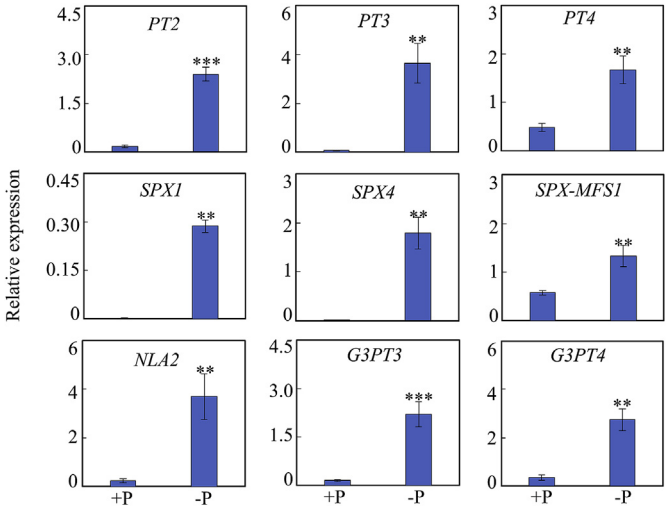

Fig. 5. Validation of transcription of identified DEGs related to Pi homeostasis in qRT-PCR analysis of soybean roots. The tested DEGs include *PT2/3/4* (*phosphate transporter 2/3/4*), *SPX1/4* (*SPX domain-containing gene 1/4*), *SPX-MFS1* (*major facilitator superfamily with SPX domain-containing protein 1*), *NLA2* (*nitrogen limitation adaptation 2*), *G3PT3/4* (*glycerol-3-phosphate transporter 3/4*). Data are means of four replicates with standard error bars. Asterisks indicate significant difference between high P (+P) and low P (-P) treatments in the Student's t-test (**: $P < 0.01$; ***: $P < 0.001$).

starvation are regulated by complex regulatory networks.

3.9. DEGs participating in nucleotide metabolisms

A total of 26 DEGs were identified to be associated with nucleotide metabolisms through KEGG analysis, including purine and pyrimidine metabolisms (Table S12). Among them, fourteen DEGs were tightly integrated into metabolism processes of purines with differential accumulation, such as IMP, AMP, 3′-AMP, GMP, inosine, deoxyguanosine, and deoxyadenosine (Fig. S4). Increased transcription of *ribonucleoside-diphosphate reductase subunit M2* (*RRM2*) and *nucleoside-diphosphate kinase* (*NDK*) seemed to be associated with significant increases of deoxyguanosine in soybean roots at low P levels (Fig. S4). Meanwhile, increased transcription of *adenylate kinase* (*AK*) appeared to be related to significant increases of deoxyadenosine and deoxyinosine in soybean roots by Pi starvation (Fig. S4). This suggests that the DEGs might function in the observed accumulation of certain metabolites associated with nucleotide metabolisms.

3.10. Validation of gene transcription using qRT-PCR

To confirm RNA-seq results, qRT-PCR analysis of 21 DEGs was further conducted using soybean roots grown at two P levels. The tested genes included nine functioning in Pi homeostasis, two genes acting in flavonoid metabolism, two functioning in phenylpropanoid metabolism, five functioning in nucleotide metabolism, and three acting in amino acid metabolisms. In qRT-PCR observations, Pi starvation in soybean roots led to enhanced transcription of nine genes involved in Pi

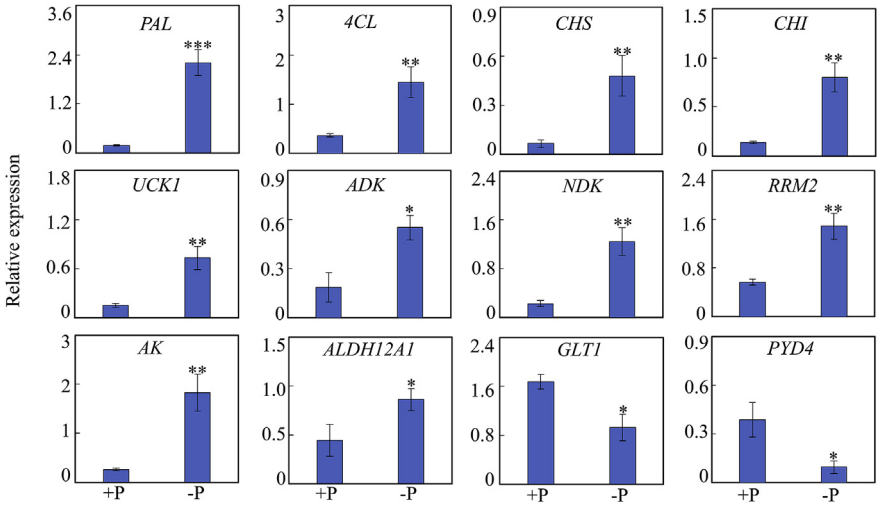

Fig. 6. Expression of DEGs related to flavonoid, nucleic acid, amino acid and phenylpropanoid metabolism as determined by qRT-PCR analysis of soybean roots. Phenylpropanoid metabolism related genes include *PAL* (*phenylalanine ammonia-lyase*), and 4CL (*4-coumarate CoA ligase*). Genes associated with flavonoid metabolism include *CHS* (*chalcone synthase)*, and *CHI* (*chalcone isomerase*). Nucleic acid metabolism genes include *UCK1* (*uridine kinase*), *ADK* (*adenosine kinase*), *NDK* (*nucleoside-diphosphate kinase*), *RRM2* (*ribonucleoside-diphosphate reductase subunit M2*), and *AK* (*adenylate kinase*). Amino acid metabolism genes include *ALDH12A1* (*aldehyde dehydrogenase 12A1*), *GLT1* (*NADH-dependent glutamate synthase 1*), and *PYD4* (*pyrimidine 4*). Data are means of four replicates with standard error bars. Asterisks indicate significant difference between high P (+P) and low P (-P) treatments in the Student's t-test (*: $P < 0.05$; **: $0.001 < P < 0.01$; ***: $P < 0.001$).

homeostasis, including *PT2/3/4*, *SPX1/4*, *SPX-MFS1* (*major facilitator superfamily with SPX domain-containing protein 1*), *NLA2* (*nitrogen limitation adaptation 2*), and *G3PT3/4* (Fig. 5), which was consistent with results from RNA-seq analysis (Table 3). Similarly, increased transcription in response to P deficiency was also observed for *PAL* (*phenylalanine ammonia-lyase*) and 4CL (*4-coumarate CoA ligase*), both of which function in the phenylpropanoid metabolism, as well as, *CHS* and *CHI*, which act in flavonoid metabolism (Fig. 6). Meanwhile, expression levels of *ADK* (*adenosine kinase*), *NDK* (*nucleoside-diphosphate kinase*), *AK* (*adenylate kinase*), and *RRM2* (*ribonucleoside-diphosphate reductase subunit M2*) from purine metabolism pathways, and *UCK1* (*uridine kinase*), which acts in pyrimidine metabolism, all increased in soybean roots responding to Pi starvation (Fig. 6). For DEGs involved in amino acid metabolism, *ALDH12A1* was significantly up-regulated, while *PYD4* (*pyrimidine 4*) and *GLT1* were significantly down-regulated by Pi starvation (Fig. 6), which was consistent with the results from RNA-seq analysis.

4. Discussion

Low Pi availability constrains crop growth and productivity, especially in acid soils, in which applied Pi fertilizers are easily fixed by soil particles into forms unavailable to crops (Kochian et al., 2015). In many situations around the world, sustainable agriculture development will include breeding cultivars with high P efficiency, which, in turn requires further understanding of morphological, physiological, and molecular mechanisms underlying plant adaptations to P deficiency (Chiou and Lin, 2011; Liang et al., 2014; Chen and Liao, 2017; Ham et al., 2018). In recent decades, identification and functional characterization of Pi starvation responsive genes has shed light on molecular mechanisms underlying plant adaptations to limited Pi availability (Chiou and Lin, 2011; Liang et al., 2014; Ham et al., 2018). More recently, expanded transcriptomic and metabolomic analyses have allowed for genomic scale mapping of complex plant responses to Pi starvation (Secco et al., 2013; Müller et al., 2015; Pant et al., 2015). However, few studies have included simultaneously observed metabolomes and transcriptomes, or tried to integrate transcriptome data with metabolome analysis. In this study, the molecular responses of soybean to Pi starvation have for the first time been investigated through integrated genome-wide transcriptome and metabolome analyses, which resulted in suggesting novel adaptive strategies of soybean for further investigation.

Remobilization of internal phosphorylated metabolites (e.g., nucleic acids, phospholipids and phosphorylated carbon) is well documented as a typical strategy employed by plant adapted to P deficiency (Plaxton and Tran, 2011; Pant et al., 2015). As a consequence, the accumulation of sets of phosphorylated molecules declined dramatically in responses to P deficiency in order to optimize internal Pi utilization (Plaxton and Tran, 2011; Müller et al., 2015; Pant et al., 2015). For example, it has been documented that Pi starvation results in the replacement of phospholipids by amphipathic sulfolipids and galactolipids in biomembranes in plants (Plaxton and Tran, 2011). Similarly, the accumulation of 23 metabolites associated with glycerophospholipid metabolism decreased significantly in soybean roots under low P conditions (Table 2). This strongly supports the conclusion that metabolic processes involving the phospholipids are dramatically remodeled by Pi starvation in soybean roots. This was further supported in the observation that sets of genes acting in phospholipid degradation and synthesis were up-regulated and down-regulated, respectively, by Pi starvation in soybean, with perhaps the most notable being up-regulated *phospholipase Ds* (*PLDs, Glyma.20G238000*, *Glyma.14G139200*) (Table S7). At the same time, Pi starvation significantly enhanced the transcription of genes involved in amphipathic sulfolipid and galactolipid metabolisms, such as *sulfoquinovosyldiacylglycerol* (*SQD, Glyma.03G131100*, *Glyma.19G133100*, *Glyma.01G113000* and *Glyma.03G078300*) (Table S7). Similarly, differential expression of genes involved in phosphide metabolic processes has been widely identified through genome-wide transcriptome analysis in plants responsive to Pi starvation, such as rice and soybean (Secco et al., 2013; Xue et al., 2018). Furthermore, it has recently been documented that the Pi starvation responsive genes *PPsPase1* and *PECP1* participate in the hydrolysis of two key components of biomembranes in Arabidopsis, phosphorylethanolamine and phosphocholine (Tannert et al., 2017). In the present study, significant decreases of both phosphorylethanolamine and phosphocholine were also observed in soybean roots grown at low P levels (Table 2). Plus, homologues of *PPsPase1* and *PECP1* were also found to be up-regulated by Pi starvation in soybean roots, including *Glyma.07G011800*, *Glyma.07G011900*, *Glyma.08G195000* and *Glyma.08G195100* (Table S7), strongly suggesting that these genes might control phosphorylethanolamine and phosphocholine hydrolysis in soybean roots under low P conditions, which merits further functional analysis.

In plant cells, phosphorylated nucleic acids are the largest organic P pool (Veneklaas et al., 2012). Therefore, it has been suggested that Pi starvation might both inhibit synthesis and promote degradation of phosphorylated nucleic acids. In one example, nucleic acid concentration in white lupin declined with decreasing Pi availability (Müller et al., 2015). Similarly, in the present study, the concentrations of ten phosphorylated nucleic acids declined in soybean roots under Pi starvation conditions (Table 2), strongly hinting that metabolic processes involving phosphorylated nucleic acids are dramatically influenced in soybean roots responding to Pi starvation. Furthermore, a set of genes

involved in metabolic processes of nucleic acids were either up-regulated or down-regulated by P deficiency (Table S12). For example, transcription of a *nucleoside diphosphate kinase* (*NDK*, *Glyma.08G022500*), which catalyzes diphosphate nucleosides into triphosphate nucleosides, increased significantly in response to Pi starvation in soybean roots (Table S12). Similarly, organelle exonuclease, DPD1 has been suggested to participate in degradation of organic DNA (Takami et al., 2018). Phosphorus deficiency led to increased transcription of *DPD1* homologues in soybean, including *Glyma.16G052000* and *Glyma.19G098500* (Table S7). Although the functions of most DEGs involved in metabolic processes of phosphorylated nucleic acids remain largely unknown in soybean, changes of their expression patterns and associated quantities of phosphorylated nucleic acids in soybean roots strongly suggest that phosphorylated nucleic acids might act as pool of organic P that contributes to Pi remobilization in soybean subjected to P deficiency.

Flavonoids, one of the largest groups of secondary metabolites participate in diverse biological activities in plants, such as protection against ultraviolet-B and root development (Tohge et al., 2017; Tan et al., 2019). More flavonoid-related metabolites were affected by Pi starvation in soybean than has been reported in other plant species, with 26 flavonoid metabolites responding to P deficiency in soybean roots compared to 7 in Arabidopsis and 2 in white lupin (Table S5; Müller et al., 2015; Pant et al., 2015). The results herein suggest that processes related to flavonoid metabolism might be dramatically modulated by Pi starvation in soybean. One type of flavonoids, anthocyanin, is commonly observed in plant leaves or shoots under low P conditions (Müller et al., 2015; Pant et al., 2015). Not surprisingly, a set of flavonoids associated with anthocyanin metabolic processes responded in this study to P deprivation. Similarly, differential accumulation of three anthocyanin-related metabolites (i.e., malvin, peonidin O-hexoside and peonidin O-malonylhexoside) was identified in soybean roots, strongly suggesting that metabolic processes associated with anthocyanins might also be modulated in soybean roots by Pi starvation. Consistently, a set of genes involved in flavonoid metabolism, such as *CHS*, *CHR*, *CHI*, *F3′H* and *LAR*, were found to be differentially regulated by Pi starvation (Fig. 3). Among the diversity of functions putatively filled by flavonoids in plants, it has been suggested that increased accumulation of anthocyanins in leaves or shoots could have a photoprotective function (Zeng et al., 2010). In roots, the functions of anthocyanins remain to be clarified. It has been suggested root-secreted flavonoids not only to delay the microbial degradation of secreted organic acids, but also to facilitate rhizosphere Pi mobilization (Tomasi et al., 2008). Furthermore, it has been documented that flavonoids might influence root growth mainly through disturbing auxin gradient in root tips (Grunewald et al., 2012). Though specific roles for flavonoids were not defined in this study, those exhibiting differential accumulation in response to Pi availability suggest that soybean root flavonoid responses to P deprivation warrant further in-depth study.

Consistent with previous studies, enhanced root growth is generally observed by short-term Pi starvation in many plant species, as reflected by increases of lateral number and length, root hair density and length (Chiou and Lin, 2011; Liang et al., 2014). In the study, it was observed that soybean root growth was increased after 9 and 12 d of Pi starvation (Fig. 1), strongly suggesting that differential accumulation of genes or metabolites might contribute to enhancement of root growth in soybean under low P conditions. For example, it was found that elongation of primary and adventitious roots was improved in rice *leaf tip necrosis 1* (i.e., *ltn1*) mutants under low P conditions, suggesting that *LTN1* mediates root responses to Pi starvation (Hu et al., 2011). Consistently, homologues of *LTN1*, were found to be down-regulated by Pi starvation in soybean roots, including *Glyma.13G179600*, *Glyma.13G239100* and *Glyma.07G196500* (Table S7). Meanwhile, two *glycerophosphodiester phosphodiesterases* (i.e., *GPX-PDE1* and *GPX-PDE2*) have been found to play a role in root hair growth in white lupin (Cheng et al., 2011). Similarly, homologues of *GPX-PDE1/2* were up-regulated by Pi starvation in soybean roots, including *Glyma.05G020500* and *Glyma.16G052000* (Table S7). Though specific roles for DEGs associated with root growth were not characterized in this study, those exhibiting differential expression patterns in response to Pi availability suggests that they merit further in-depth study.

5. Conclusions

In this study, global transcriptome and metabolome analyses were conducted simultaneously and integrated to shed light on molecular mechanisms underlying soybean root adaptations to Pi starvation. Identification of Pi starvation responsive metabolites, especially for phosphorylated lipids and nucleic acids, hinted adaptive strategies employed by soybean roots responding to Pi starvation. One known strategy is scavenging of internal Pi from phosphorylated metabolites, which was observed in our experiment, as well as differential expression of many types of genes and variation in the accumulation of a range of P related metabolites. On the whole, this study contributes to understanding of diverse plant responses and adaptations to Pi starvation. Furthermore, identified DEGs will provide potential target region for future efforts to develop P-efficient soybean cultivars through marker-assisted breeding and genetic engineering.

Conflicts of interest

The authors declare that they have no competing interests.

Authors' contributions

JT, CL, XM conceived and designed the experiments. XM, MZ and LC performed the experiments. XM, MZ, LC, CL and JT analyzed the data. XM, JT and CL wrote the manuscript. All authors have read and approved the final manuscript.

Acknowledgement

This research was funded by the National Natural Science Foundation of China (31872164 and 31672220), Integrated Demonstration of Key Techniques for the Industrial Development of Featured Crops in Rocky Desertification Areas of Yunnan-Guangxi-Guizhou Provinces, Guangdong Natural Science Funds for Distinguished Young Scholars (2015A030306034), the High Level Talents Special Support Plan of Guangdong Province (2015T×01N042 and 2015TQ01N078). We thank Dr. Thomas Walk for critically reading the manuscript.

Appendix A. Supplementary data

Supplementary data to this article can be found online at https://doi.org/10.1016/j.plaphy.2019.04.033.

References

Abel, S., 2017. Phosphate scouting by root tips. Curr. Opin. Plant Biol. 39, 168–177.
Chen, L., Liao, H., 2017. Engineering crop nutrient efficiency for sustainable agriculture. J. Integr. Plant Biol. 59, 710–735.
Chen, W., Gong, L., Guo, Z., Wang, W., Zhang, H., Liu, X., Yu, S., Xiong, L., Luo, J., 2013. A novel integrated method for large-scale detection, identification, and quantification of widely targeted metabolites: application in the study of rice metabolomics. Mol. Plant 6, 1769–1780.
Chen, Z., Cui, Q., Liang, C., Sun, L., Tian, J., Liao, H., 2011. Identification of differentially expressed proteins in soybean nodules under phosphorus deficiency through proteomic analysis. Proteomics 11, 4648–4659.
Cheng, L., Bucciarelli, B., Liu, J., Zinn, K., Miller, S., Patton-Vogt, J., Allan, D., Shen, J., Vance, C.P., 2011. White lupin cluster root acclimation to phosphorus deficiency and root hair development involve unique glycerophosphodiester phosphodiesterases. Plant Physiol. 156, 1131–1148.
Chiou, T.J., Lin, S.I., 2011. Signaling network in sensing phosphate availability in plants. Annu. Rev. Plant Biol. 62, 185–206.

Giri, J., Bhosale, R., Huang, G., Pandey, B.K., Parker, H., Zappala, S., Yang, J., Dievart, A., Bureau, C., Ljung, K., Price, A., Rose, T., Larrieu, A., Mairhofer, S., Sturrock, C.J., White, P., Dupuy, L., Hawkesford, M., Perin, C., Liang, W., Peret, B., Hodgman, C.T., Lynch, J., Wissuwa, M., Zhang, D., Pridmore, T., Mooney, S.J., Guiderdoni, E., Swarup, R., Bennett, M.J., 2018. Rice auxin influx carrier OsAUX1 facilitates root hair elongation in response to low external phosphate. Nat. Commun. 9, 1408.

Guo, W., Zhao, J., Li, X., Qin, L., Yan, X., Liao, H., 2011. A soybean β-expansin gene GmEXPB2 intrinsically involved in root system architecture responses to abiotic stresses. Plant J. 66, 541–552.

Grunewald, W., De Smet, I., Lewis, D.R., Löfke, C., Jansen, L., Goeminne, G., Bossche, R.V., Karimi, M., Rybel, B.D., Vanholme, B., Teichmann, T., Boerjan, W., Montagu, M.V., Gheysen, G., Muday, G.K., Friml, J., Beeckman, T., 2012. Transcription factor WRKY23 assists auxin distribution patterns during Arabidopsis root development through local control on flavonol biosynthesis. Proc. Natl. Acad. Sci. U. S. A 109, 1554–1559.

Ham, B.K., Chen, J., Yan, Y., Lucas, W.J., 2018. Insights into plant phosphate sensing and signaling. Curr. Opin. Biotechnol. 49, 1–9.

Hernández, G., Ramírez, M., Valdés-López, O., Tesfaye, M., Graham, M.A., Czechowski, T., Schlereth, A., Wandrey, M., Erban, A., Cheung, F., Wu, H.C., Lara, M., Town, C.D., Kopka, J., Udvardi, M.K., Vance, C.P., 2007. Phosphorus stress in common bean: root transcript and metabolic responses. Plant Physiol. 144, 752–767.

Hernández, G., Valdés-López, O., Ramírez, M., Goffard, N., Weiller, G., Aparicio-Fabre, R., Fuentes, S.I., Erban, A., Kopka, J., Udvardi, M.J., Vance, C.P., 2009. Global changes in the transcript and metabolic profiles during symbiotic nitrogen fixation in phosphorus-stressed common bean plants. Plant Physiol. 151, 1221–1238.

Herridge, D.F., Peoples, M.B., Boddey, R.M., 2008. Global inputs of biological nitrogen fixation in agricultural systems. Plant Soil 311, 1–18.

Hu, B., Zhu, C., Li, F., Tang, J., Wang, Y., Lin, A., Liu, L., Che, R., Chu, C., 2011. LEAF TIP NECROSIS1 plays a pivotal role in the regulation of multiple phosphate starvation responses in rice. Plant Physiol. 156, 1101–1115.

Kim, D., Langmead, B., Salzberg, S.L., 2015. HISAT: a fast spliced aligner with low memory requirements. Nat. Methods 12, 357.

Kochian, L.V., Piñeros, M.A., Liu, J., Magalhaes, J.V., 2015. Plant adaptation to acid soils: the molecular basis for crop aluminum resistance. Annu. Rev. Plant Biol. 66, 571–598.

Li, C., Gui, S., Yang, T., Walk, T., Wang, X., Liao, H., 2012. Identification of soybean purple acid phosphatase genes and their expression responses to phosphorus availability and symbiosis. Ann. Bot. 109, 275–285.

Li, B., Dewey, C.N., 2011. RSEM: accurate transcript quantification from RNA-Seq data with or without a reference genome. BMC Bioinf. 12, 1–16.

Li, S., Dong, X., Fan, G., Yang, Q., Shi, J., Wei, W., Zhao, F., Li, N., Wang, X., Wang, F., Feng, X., Zhang, X., Song, G., Shi, G., Zhang, W., Qiu, F., Wang, D., Li, X., Zhang, Y., Zhao, Z., 2018. Comprehensive profiling and inheritance patterns of metabolites in foxtail millet. Front. Plant Sci. 9, 1716 1716.

Li, X., Zhao, J., Tan, Z., Zeng, R., Liao, H., 2015. GmEXPB2, a cell wall β-expansin, affects soybean nodulation through modifying root architecture and promoting nodule formation and development. Plant Physiol. 169, 2640–2653.

Liang, C., Piñeros, M.A., Tian, J., Yao, Z., Sun, L., Liu, J., Shaff, J., Coluccio, A., Kochian, L.V., Liao, H., 2013. Low pH, aluminum, and phosphorus coordinately regulate malate exudation through GmALMT1 to improve soybean adaptation to acid soils. Plant Physiol. 161, 1347–1361.

Liang, C., Wang, J., Zhao, J., Tian, J., Liao, H., 2014. Control of phosphate homeostasis through gene regulation in crops. Curr. Opin. Plant Biol. 21, 59–66.

Liese, R., Schulze, J., Cabeza, R.A., 2017. Nitrate application or P deficiency induce a decline in *Medicago truncatula* N2-fixation by similar changes in the nodule transcriptome. Sci. Rep. 7, 46264.

Mehra, P., Pandey, B.K., Verma, L., Giri, J., 2018. A novel glycerophosphodiester phosphodiesterase improves phosphate deficiency tolerance in rice. Plant Cell Environ. 42, 1167–1179.

Mora-Macías, J., Ojeda-Rivera, J.O., Gutiérrez-Alanís, D., Yong-Villalobos, L., Oropeza-Aburto, A., Raya-González, J., Jiménez-Domínguez, G., Chávez-Calvillo, G., Rellán-Álvarez, R., Herrera-Estrella, L., 2017. Malate-dependent Fe accumulation is a critical checkpoint in the root developmental response to low phosphate. Proc. Natl. Acad. Sci. U. S. A 114, 3563–3572.

Müller, J., Gödde, V., Niehaus, K., Zörb, C., 2015. Metabolic adaptations of white lupin roots and shoots under phosphorus deficiency. Front. Plant Sci. 6, 1014.

Murphy, J., Riley, J., 1962. A modified single solution method for the determination of phosphate in natural water. Anal. Chim. Acta 127, 31–36.

Plaxton, W.C., Tran, H.T., 2011. Metabolic adaptations of phosphate-starved plants. Plant Physiol. 156, 1006–1015.

Pant, B.D., Pant, P., Erban, A., Huhman, D., Kopka, J., Scheible, W.R., 2015. Identification of primary and secondary metabolites with phosphorus status-dependent abundance in Arabidopsis, and of the transcription factor PHR1 as a major regulator of metabolic changes during phosphorus limitation. Plant Cell Environ. 38, 172–187.

Peng, W., Wu, W., Peng, J., Li, J., Lin, Y., Wang, Y., Tian, J., Sun, L., Liang, C., Liao, H., 2018. Characterization of the soybean GmALMT family genes and the function of *GmALMT5* in response to phosphate starvation. J. Integr. Plant Biol. 60, 216–231.

Qin, L., Jiang, H., Tian, J., Zhao, J., Liao, H., 2011. Rhizobia enhance acquisition of phosphorus from different sources by soybean plants. Plant Soil 349, 25–36.

Qin, L., Zhao, J., Tian, J., Chen, L., Sun, Z., Guo, Y., Lu, X., Gu, M., Xu, G., Liao, H., 2012. The high-affinity phosphate transporter GmPT5 regulates phosphate transport to nodules and nodulation in soybean. Plant Physiol. 159, 1634–1643.

Secco, D., Jabnoune, M., Walker, H., Shou, H., Wu, P., Poirier, Y., Whelan, J., 2013. Spatio-temporal transcript profiling of rice roots and shoots in response to phosphate starvation and recovery. Plant Cell 25, 4285–4304.

Tannert, M., May, A., Ditfe, D., Berger, S., Balcke, G.U., Tissier, A., Köck, M., 2017. Pi starvation-dependent regulation of ethanolamine metabolism by phosphoethanolamine phosphatase PECP1 in Arabidopsis roots. J. Exp. Bot. 69, 467–481.

Takami, T., Ohnishi, N., Kurita, Y., Iwamura, S., Ohnishi, M., Kusaba, M., Mimura, T., Sakamoto, W., 2018. Organelle DNA degradation contributes to the efficient use of phosphate in seed plants. Native Plants 4, 1044–1055.

Tan, H., Man, C., Xie, Y., Yan, J., Chu, J., Huang, J., 2019. A crucial role of GA-regulated flavonol biosynthesis in root growth of Arabidopsis. Mol. Plant 12, 521–537.

Tarazona, S., García-Alcalde, F., Dopazo, J., Ferrer, A., Conesa, A., 2011. Differential expression in RNA-seq: a matter of depth. Genome Res. 21, 2213–2223.

Tian, J., Wang, X., Tong, Y., Chen, X., Liao, H., 2012. Bioengineering and management for efficient phosphorus utilization in crops and pastures. Curr. Opin. Biotechnol. 23, 866–871.

Tohge, T., de Souza, L.P., Fernie, A.R., 2017. Current understanding of the pathways of flavonoid biosynthesis in model and crop plants. J. Exp. Bot. 68, 4013–4028.

Tomasi, N., Weisskopf, L., Renella, G., Landi, L., Pinton, R., Varanini, Z., Nannipieri, P., Torrent, J., Martinoia, E., Cesco, S., 2008. Flavonoids of white lupin roots participate in phosphorus mobilization from soil. Soil Biol. Biochem. 40, 1971–1974.

Veneklaas, E.J., Lambers, H., Bragg, J., Finnegan, P.M., Lovelock, C.E., Plaxton, W.C., Price, C.A., Scheible, W., Shane, M.W., White, P.J., Raven, J.A., 2012. Opportunities for improving phosphorus-use efficiency in crop plants. New Phytol. 195, 306–320.

Wu, W., Lin, Y., Liu, P., Chen, Q., Tian, J., Liang, C., 2018. Association of extracellular dNTP utilization with a GmPAP1-like protein identified in cell wall proteomic analysis of soybean roots. J. Exp. Bot. 69, 603–617.

Wang, Y., Lysøe, E., Armarego-Marriott, T., Erban, A., Paruch, L., Eerde, A., Bock, R., Liu-Clarke, J., 2018. Transcriptome and metabolome analysis provide insights into root and root released organic anion responses to phosphorus deficiency in oat. J. Exp. Bot. 69, 3759–3771.

Wang, Z., Ruan, W., Shi, J., Zhang, L., Xiang, D., Yang, C., Li, C., Wu, Z., Liu, Y., Yu, Y., Shou, H., Mo, X., Mao, C., Wu, P., 2014. Rice SPX1 and SPX2 inhibit phosphate starvation responses through interacting with PHR2 in a phosphate-dependent manner. Proc. Natl. Acad. Sci. U. S. A 111, 14953–14958.

Xu, F., Liu, Q., Chen, L., Kuang, J., Walk, T., Wang, J., Liao, H., 2013. Genome-wide identification of soybean microRNAs and their targets reveals their organ-specificity and responses to phosphate starvation. BMC Genomics 14, 66.

Xu, L., Zhao, H., Wan, R., Liu, Y., Xu, Z., Tian, W., Ruan, W., Wang, F., Deng, M., Wang, J., Dolan, L., Luan, S., Xue, S., Yi, K., 2019. Identification of vacuolar phosphate efflux transporters in land plants. Native Plants 5, 84–94.

Xue, Y.B., Xiao, B.X., Zhu, S.N., Mo, X.H., Liang, C.Y., Tian, J., Liao, H., 2017. GmPHR25, a GmPHR member up-regulated by phosphate starvation, controls phosphate homeostasis in soybean. J. Exp. Bot. 68, 4951–4967.

Xue, Y.B., Zhuang, Q.L., Zhu, S.N., Xiao, B.X., Liang, C.Y., Liao, H., Tian, J., 2018. Genome wide transcriptome analysis reveals complex regulatory mechanisms underlying phosphate homeostasis in soybean nodules. Int. J. Mol. Sci. 19, 2924 2924.

Yao, Z.F., Liang, C.Y., Zhang, Q., Chen, Z.J., Xiao, B.X., Tian, J., Liao, H., 2014. SPX1 is an important component in the phosphorus signaling network of common bean regulating root growth and phosphorus homeostasis. J. Exp. Bot. 65, 3299–3310.

Zeng, X.Q., Chow, W.S., Su, L.J., Peng, X.X., Peng, C.L., 2010. Protective effect of supplemental anthocyanins on Arabidopsis leaves under high light. Physiol. Plantarum 138, 215–225.

Zhang, Z., Zheng, Y., Ham, B.K., Zhang, S., Fei, Z., Lucas, W.J., 2018. Plant lncRNAs are enriched in and move systemically through the phloem in response to phosphate deficiency. J. Integr. Plant Biol. 61, 492–508.